CCD SURFACE PHOTOMETRY OF THREE LOW-LUMINOSITY RADIO GALAXIES CONTAINING RADIO JETS1

J. I. GONZALEZ-SERRANO

Dpto. de Física Moderna, Universidad de Cantabria and Instituto de Estudios Avanzados en Física Moderna y Biologia Molecular, CSIC-Univ. de Cantabria, Avda. de los Castros s/n, E-39005 Santander, Spain

I. PEREZ-FOURNON

Instituto de Astrofisica de Canarias, E-38200 La Laguna, Tenerife, Spain Received 21 January 1992; revised 21 April 1992

ABSTRACT

We present and discuss the results of CCD photometry of the three low-luminosity radio galaxies which contain jets at the kpc scale: B2 0836+29, B2 2116+26, and B2 2236+35. We study the photometric properties of the galaxies by analyzing the radial variations of surface brightness, ellipticity, major axis position angle, and isophote center. We characterize the deviations of the isophotes from perfect elliptical contours. The morphological properties of the galaxies are discussed in terms of their local environment and radio emission. We find that the galaxies present optical peculiarities that are signatures of merging processes or interactions. By subtracting galaxy models to the original frames, the resulting residual images allow us to put limits to the radio to optical spectral indices of the jets. We infer that the synchrotron spectra of these jets have cutoff frequencies below 5×10^{14} Hz.

1. INTRODUCTION

Recent works (González-Serrano 1989; González-Serrano & Pérez-Fournon 1989; Colina & Pérez-Fournon 1990a,b; González-Serrano & Pérez-Fournon 1991, hereafter referred to as Paper I) studying the optical properties of low-luminosity radio galaxies (LLRG) have shown that a high fraction of objects have a complex, peculiar optical morphology, indicating gravitational interaction between elliptical galaxies and/or a large elliptical and a smaller disk galaxy, most probably related to the nuclear activity and jet production. Studies of powerful radio galaxies (PRG) show that a high proportion of objects present also a distorted optical morphology and that usually they appear interacting with close companions (Heckman et al. 1986; Smith & Heckman 1989a,b; Baum & Heckman 1989a,b).

On the other hand, detailed studies of nearby, bright elliptical galaxies provide evidence of deviation from ellipticity. In particular, many E galaxies present boxy isophotes (Jedrzejewski 1987; Bender et al. 1988; Nieto & Bender 1989; Peletier 1989). Basically, boxiness is quantified by measuring the amplitude of the fourth harmonic $(B_4 \text{ or } \cos 4\theta \text{ parameter})$ when the intensity along the best-fit elliptical contour fitted to a given isophote is expressed as a Fourier series of the eccentric anomaly θ . Correlations between boxiness, and the presence of x-ray and radio emission, have been found by Bender et al. (1989) and have been interpreted as due to merging processes (Nieto & Bender 1989). This claim seems to be

In this paper we present CCD imaging of the radio galaxies B2 0836+29, B2 2116+26 (NGC 7052), and B2 2236+35. This work, together with Paper I, represents the first results of a long-term project devoted to explore the properties of LLRG with radio jets of the list of Parma et al. (1987). At present, good quality data were obtained for 60% of this sample and the analysis is underway. Since LLRG usually present jets on both sides of a weak core, these objects are very suited to study the physics of extragalactic jets. Jets play a fundamental role in the transport of energy from the nucleus to the radio lobes. The understanding of the physics governing the propagation and radiation of the jets requires detailed observations to constrain the models. The jets are characterized by powerlaw spectral shapes at low frequencies (radio), implying a power-law energy distribution for the radiating electrons. Optical, infrared, and UV observations are important in determining the electron distribution at high energies. In the optical region, only a very small number of jets have been detected [see Freix-Burnet et al. (1991) and references therein], most probably due to a falloff toward high frequencies produced by a break in the electron energy spectrum. In the present study, we search for the optical counterpart of the radio jets with the aim of investigating the distribution of spectral indices and cutoff frequencies.

The paper is divided as follows: Section 2 describes the observations, and the results are presented in Sec. 3. A discussion of the results for the three galaxies together with the radio galaxies B2 0034+25 and B2 0206+35 (Paper I) is given in Sec. 4. A Hubble constant of 75 km s⁻¹ Mpc^{-1} is used throughout this paper.

supported by recent high spatial resolution observations of the core of bright E galaxies (Nieto et al. 1991) which reveal that disk-E galaxies maintain their original structure, formed by dissipative collapse, while boxy and irregular galaxies result from merger processes.

¹Based on observations made with the Isaac Newton Telescope operated by the Royal Greenwich Observatory at the Spanish Observatorio del Roque de los Muchachos of the Instituto de Astrofísica de Canarias on behalf of the Science and Engineering Research Council of the United Kingdom and the Netherlands Organization for Scientific Research (NWO).

TABLE 1. Observing log.

B2 name	α δ		t_{exp}	
	(1950)	(1950)	(s)	
0836+29	08 36 13.4	29 01 17	180, 300	
2116+26	21 16 20.7	26 14 08	100, 600	
2236+35	22 36 12.3	35 04 11	180	

2. OBSERVATIONS AND DATA REDUCTION

The three galaxies discussed here were observed on 1987 October 18 at the 2.5 m Isaac Newton Telescope (INT) of the Observatorio del Roque de los Muchachos (La Palma, Spain) using an RCA CCD camera at the prime focus which provides a pixel size of 0".74 and a field of view of $237" \times 379"$. Several exposures were obtained in a KPNO V filter. A log of the observations is given in Table 1. The seeing was in the range 1".3-2".0 full width at half-maximum (FWHM) and the observing conditions were photometric.

The procedures used for flux calibration, reductions, and photometric analysis are detailed in Paper I.

3. RESULTS

In Table 2 we list some parameters of the three radio sources discussed in this paper and give references to their main radio properties. While B2 2116+26 and B2 2236+35 are clearly of low radio luminosity, B2 0836+29 has a radio luminosity intermediate between PRG and LLRG. It also has a much larger extended radio emission than the two other B2 radio galaxies discussed here, and presents edge-brightened radio lobes. In this section we present the results of the isophote analysis and of the galaxy model subtraction for the three objects. Table 3 gives the main photometric parameters obtained from this analysis.

3.1 B2 0836 + 29

This galaxy is the brightest member of the Abell cluster A690 (richness 1). The radio source presents two lobes and a one-sided jet of size 50'' in position angle 0° , with a total size of the radio emission of 660 kpc (Owen *et al.* 1977; Valentijn 1979). The mean surface brightness of the jet is 1 mJy arcsec⁻² and the total power of the source at

TABLE 2. Main properties of the observed radio galaxies.

B2 name	zª	$P_{1.4}(total)^b$	P _{1.4} (jet) ^c	l^d	α ^{4.8ε}
(1)	(2)	(3)	(4)	(5)	(6)
0836+29	0.0790	24.98	24.10	660	_
2116+26	0.0164	22.73	22.34	26.6	0.45
2236+35	0.0277	23.72	23.41	24	0.70

a Redshift from Colla et al. 1975.

TABLE 3. Photometric parameters of the observed galaxies.

B2 name	m_V	M_V	r_e	μ_e
			kpc	mag arcsec-2
0836+29	14.26	-23.24	12.4	22.41
2116+26	11.86	-22.22	7.5	21.87
2236+35A	12.57	-22.64	13.05	22.58
2236+35B	14.31	-20.90	2.73	21.07
2236+35C	14.89	-20.33	2.08	20.86

1.4 GHz is $10^{24.98}$ W Hz⁻¹ (Parma et al. 1987). The galaxy has an associated x-ray halo with a diameter of \sim 460 kpc, comparable with the size of the radio structure (Morganti et al. 1988). The x-ray emission is elongated towards the NE and appears aligned with the major axis of the stellar light of the galaxy. Both radio lobes lie at the edge of the x-ray emission seen in the *Einstein* IPC image.

The total V magnitude, measured using an aperture of diameter 120", is 14.26 ± 0.06 , and the corresponding absolute magnitude is $M_V = -23.24$. In the V image (Fig. 1) other 20 fainter galaxies are visible in the field, with the brightest one located at 49 kpc of the nucleus of B2 0836 +29 in P.A. 209°. This galaxy has a magnitude of 16.94 ±0.04 .

We carried out the isophotal analysis of B2 0836+29 and constructed a galaxy model that was subtracted from the original image. Figure 2 shows a contour map of the central part of the residual image obtained. In this image other 6 galaxies are observed at distances $\lesssim 65$ kpc from the nucleus of B2 0836+29 with the two nearest galaxies located at 18 and 25 kpc, in P.A. 50° and 9°, respectively.

In Fig. 3 the brightness profile in the V filter and the variations with semimajor axis of position angle, ellipticity and $\cos 4\theta$ component are represented. Variations in position angle and ellipticity are present, while the absolute value of the B_4 parameter is lower than 0.5%. From this analysis we also measure an off-centering of the outermost isophotes of $\delta/a \sim 10\%$, where δ is the difference between the position of the nucleus and the center of the isophote of semimajor axis a.

The brightness profile is well fitted by a de Vaucouleurs law in the inner parts ($r\lesssim 13~\rm kpc$), but shows a very extended envelope in the outer parts, with a semimajor axis of 110 kpc at the $26^{\rm th}$ mag arcsec⁻² level. Using the parameters of the fit ($r_{\rm e}=12.4\pm0.2~\rm kpc$ and $\mu_{\rm e}=22.41\pm0.03$) we obtain a difference between calculated and measured integrated magnitudes of 0.18 mag. This corresponds to a V magnitude of 16.3 for the envelope and represents a 15% of the total luminosity of the galaxy. The light distribution of the outer parts can be fitted by a law of the form $I(r) \propto r^{\beta}$, with $\beta = -1.52$. After subtraction of the fitted de Vaucouleurs law, the surface-brightness profile of the envelope can be well represented by the law $r^{-0.8\pm0.1}$.

b Logarithm of the total radio power at 1.4 GHz in W/Hz, from Parma et al. 1987.

c Logarithm of the radio power of the jets at 1.4 GHz in W/Hz, from Parma et al. 1987.

^d Total extension of the radio emission in kpc, from Parma et al. 1987.

^e Spectral index of the jets between 1.4 and 4.8 GHz, from Morganti et al. 1987.

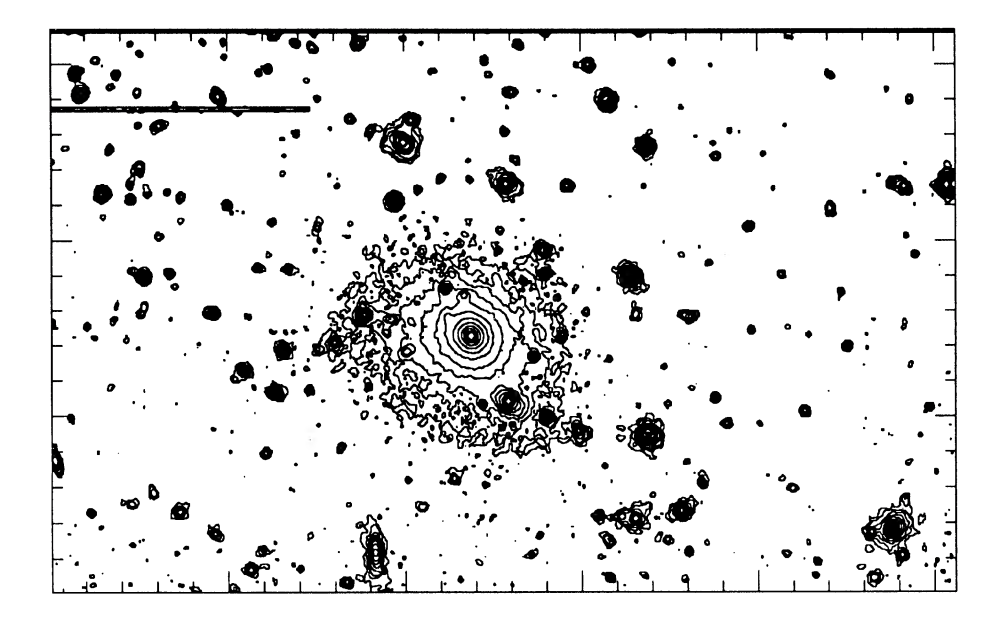


FIG. 1. Contour map of the optical counterpart of the radio galaxy B2 0836+29 in the V filter. The lowest contours represent 26.0 mag arcsec⁻². The interval between contours is 0.5 mag. North is up, east is to the left, and the separation between tick marks corresponds to 14%.

3.2 B2 2116+26 (NGC 7052)

VLA maps of B2 2116+26 at 1.4 and 4.8 GHz show a two-sided jet with a total length of 26.6 kpc in position angles 21°-201° (Morganti et al. 1987). The mean surface brightness of the northern and southern jets are 20 and 35 mJy arcsec⁻² at 1.4 GHz, respectively. Figure 4 shows the optical counterpart of this radio galaxy in the V band. The total integrated magnitude is 11.86 ± 0.06 corresponding to an absolute magnitude of -22.22. Note the box-shaped morphology of the galaxy.

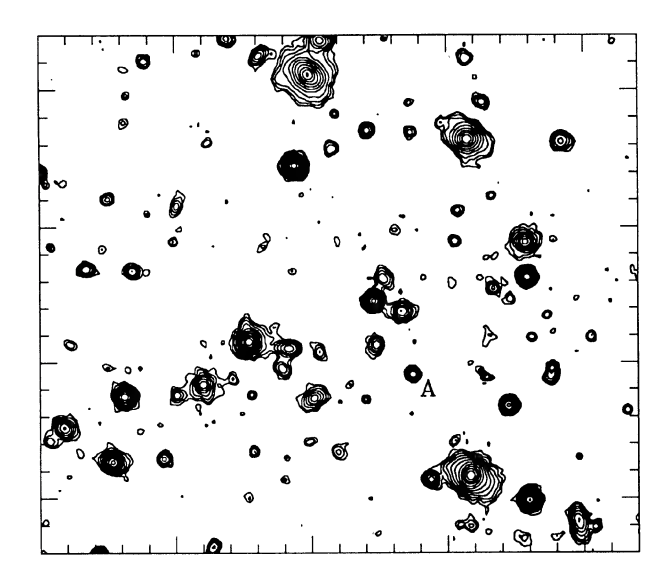


FIG. 2. Residual image of B2 0836+29 after model subtraction. The interval between contours is 0.5 mag, being the lowest contour of 25.6 mag arcsec². Letter A indicates the position of the nucleus. The separation between tick marks corresponds to 7".4.

In Fig. 5 we show a contour plot of the residual image resulting after the subtraction of the model obtained from the isophote analysis. The X-shaped residuals appear as a consequence of the high negative $\cos 4\theta$ amplitude of the outer isophotes. The object detected 9" south from the nucleus has a V magnitude of 20.3 ± 0.2 . The cos 4θ component of the isophotes becomes high at radii larger than ~28", therefore, this object is not a spurious residual caused by the boxy-shaped isophotes. The emission is not exactly coincident with, but approximately parallel to, the radio jet. The parameters of the isophotes are shown in Fig. 6 where the brightness profile is represented together with the best fit to the de Vaucouleurs law. The effective surface magnitude and effective radius are 21.87 ± 0.04 and 23.5 ± 0.4 (or 7.5 kpc) in the V band. At lower amplitude, positive $\cos 4\theta$ values are measured in the innermost region of the galaxy. The mean value of $\cos 4\theta$ at distances less than 10" is 2.6×10^{-3} , with a dispersion of 8×10^{-4} . The maximum value measured in this region is 4×10^{-3} . The radial variation of the $\cos 4\theta$ component in NGC 7052 is consistent with the data presented by Bender et al. (1988), although they covered a smaller range in distances from the nucleus. Also, our value of the half-light radius, the variation in P.A., and ellipticity are in agreement with these authors.

3.3 B2 2236+35

This radio source is located in the open cluster 2231.2 +3732 (Zwicky & Kowal 1968). B2 2236+35 has a two-sided, symmetric radio jet, with lengths of 13 and 12 kpc, in position angles 46° and 226°, respectively. The jets are embedded in a distorted low-brightness region with an S-shaped morphology. At 1.4 GHz the NE and SW jets have flux densities of 85 and 94 mJy, respectively (Morganti

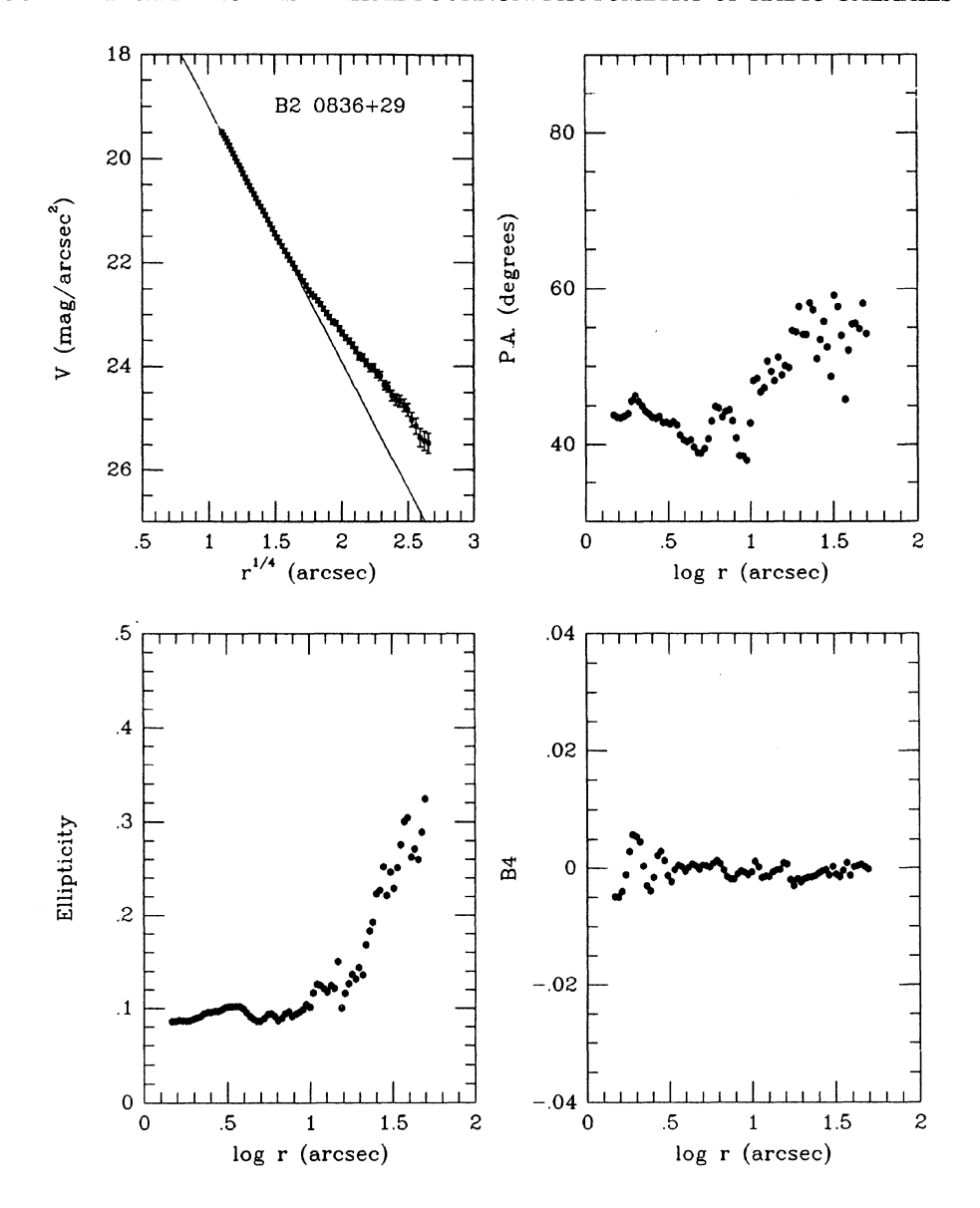


FIG. 3. Brightness profile, ellipticity, major axis position angle, and B_4 component of B2 0836+29. The solid line is the fitted de Vaucouleurs law to the inner part of the brightness profile.

et al. 1987), with a total power at this frequency of $10^{23.72}$ W Hz⁻¹ (Parma et al. 1987).

In Fig. 7 the V image of B2 2236+35 is shown. The optical counterpart of the radio source is labeled with the letter A, and with letters B and C we mark two other elliptical galaxies in the field. Other bright late-type galaxies are seen to the north of B2 2236+35, and other smaller galaxies are detected in the field. We restricted the analysis to galaxies A, B, and C. The absolute V magnitudes of the galaxies are -22.64, -20.90 and -20.33, respectively. The projected distances of the galaxies B and C to the radio source are 47.0 and 75.2 kpc, respectively.

Figure 8 shows a contour map of the residual image resulting after the subtraction of the model of the main galaxy. Three faint galaxies are detected in the residual map. We detect also an extension to the west of galaxy B,

which could be a faint galaxy. This is indicated by an arrow in Fig. 8. The parameters of the isophotes of the three galaxies are presented in Fig. 9. Galaxies B and C show excesses over the de Vaucouleurs law that fitted the inner parts of their brightness profiles, which start to deviate from the fits at radii $1.4r_{\rm e}$ and $2.8r_{\rm e}$. The integrated excesses over the fitted $r^{1/4}$ law are of 0.26 and 0.10 mag for galaxies B and C, respectively. The isophotes of the companion galaxies show twisting of $\sim 20^{\circ}$ toward the radio galaxy which shows oscillations in P.A. of $\sim 2^{\circ}$ in amplitude over radial distances of 1–2 kpc. As discussed in Paper I, the semimajor axis profiles of ellipticity, position angle, and isophote center of the galaxies in a pair must be interpreted carefully at large radii, because of the method used. Nevertheless, it was also noted that the surface-

539

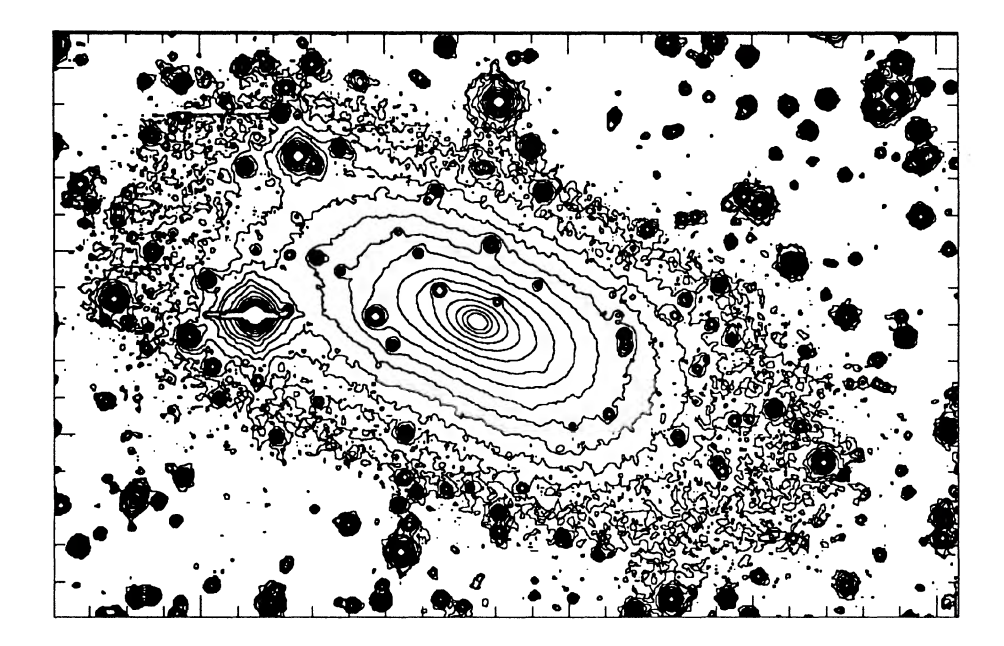


Fig. 4. Contour map of B2 2116+26 (NGC 7052) in the V filter. The lowest contour represents 25.8 mag arcsec⁻². The interval between contour is 0.5 mag. Orientation and scale are as in Fig. 1.

brightness profiles are reliable even at low intensity levels ($\sim 1.5\%$ of the sky background).

4. DISCUSSION AND CONCLUSIONS
4.1 Optical Morphology of the Radio Galaxies
4.1.1 B2 0836+29

The presence of an extended envelope with a surfacebrightness profile that follows a power law with index -1.5 and the location of the galaxy in the cluster peak, allows us to conclude that B2 0836+29 is a cD galaxy.

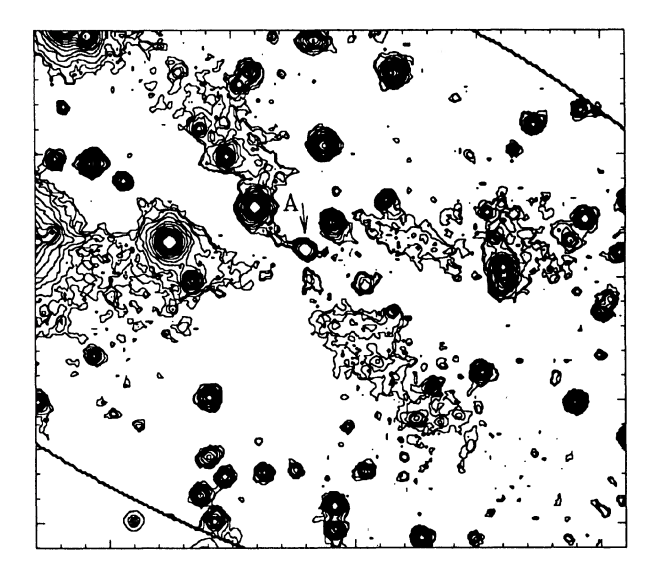


FIG. 5. Residual image of B2 2116+26 after model subtraction. The interval between contours is 0.5 mag, and the lowest contour represents 26.2 mag arcsec². Letter A indicates the position of the nucleus. The separation between tick marks corresponds to 7.4.

These properties match the criterion of Schombert (1987) in classifying brightest cluster members (BCM) and giant ellipticals by means of their morphology and surface-brightness profile. The total and envelope luminosities, as well as the effective surface magnitude and radius, are consistent with the relations found by Schombert (1988) between these parameters in cD galaxies in Abell clusters.

Ostriker & Tremaine (1975) suggested that the central galaxy in a cluster may grow into a cD galaxy by cannibalizing nearby galaxies. The fact that cD galaxies are flatter than normal ellipticals and tend to align with the axis of the cluster (Binggeli 1982) has been taken as an evidence of this process. A more direct indication of cannibalism of cluster members by first-ranked galaxies has been shown by Lauer (1988) who observes that 50% of a sample of multiple-nucleus brightest galaxies in Abell clusters present morphological perturbations originated by gravitational interaction; in particular, ~65% of the interacting systems show nonconcentric isophotes. This effect has also been found in interacting B2 radio galaxies (Paper I) and in paired elliptical galaxies (Davoust & Prugniel 1988), and is the strongest evidence for components in tidal contact.

B2 0836+29 has two nearby galaxies at projected distances of 18 and 25 kpc from the nucleus, which are comparable to the distances of the secondary nuclei in Lauer's sample. The isophote off-centering found in this galaxy appears to be, therefore, a clear evidence of cannibalism of cluster members.

On the other hand, x-ray and optical observations indicate that large amounts of gas are cooling and flowing into the centers of clusters of galaxies. It has been proposed that such cooling flows can form low mass stars and produce the growth of cD's (Fabian *et al.* 1982). The x-ray lumi-

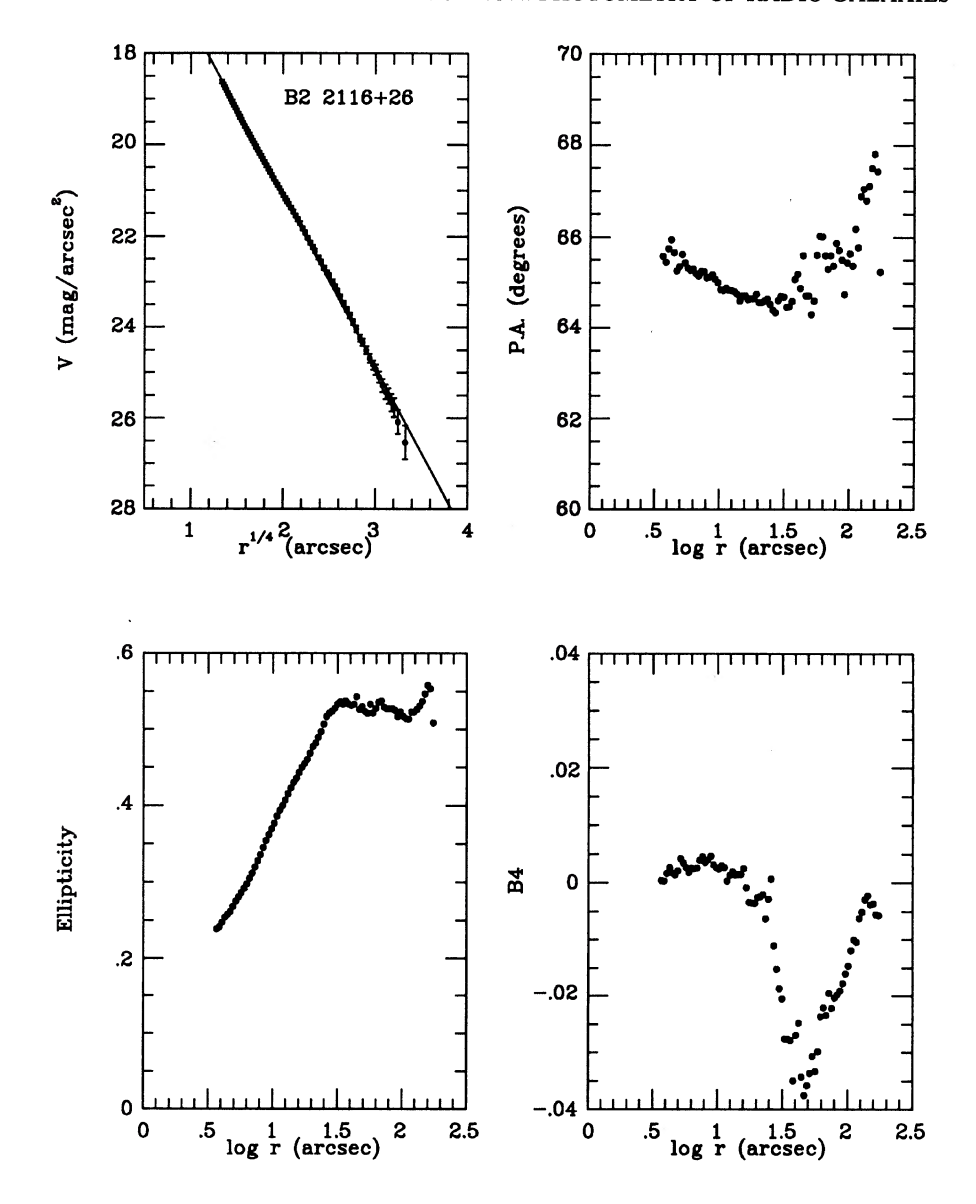


FIG. 6. Surface-brightness profile and isophote parameters of B2 2116+26. The solid line is the fitted de Vaucouleurs law.

nosity of B2 0836+29 is 7.5×10^{12} ergs s⁻¹ (Morganti et al. 1988), and the estimated central density and temperature of the gas are 9×10^{-4} cm⁻³ and 2.2×10^{7} K, respectively. Using these data, we estimate that the cooling time in B2 0836+29 is $t_{\rm cool}\sim4\times10^{10}$ yr, which is too high for cooling flow related growth to be important. In conclusion, the accretion of the hot gas around 0836+29 in the form of cooling flows seems negligible and, therefore, the most probable mechanism for accreting mass in this case is by cannibalizing nearby cluster members.

4.1.2 B2 2116+26

NGC 7052 presents a high negative $\cos 4\theta$ component at radii larger than 28". The residuals (Fig. 5) show clearly the effect of the boxiness. The high radial increase in ellipticity and the constant position angle of the iso-

photes are indicative of a prolate intrinsic structure. This is reinforced by the presence of minor axis rotation, as reported by Wagner *et al.* (1988).

The positive $\cos 4\theta$ component found in the inner part of NGC 7052 can be attributed to the presence of a stellar disk. In addition, a nuclear, small dust lane has been reported in NGC 7052 by Gallagher (1986), which could be responsible for the *IRAS* emission detected in this galaxy at 60 and 100 μ m (Jura 1986). This dust lane is not detected in our image, most probably because of the low spatial resolution and inappropriate sampling of the CCD camera at the prime focus. The boxy structure and the presence of dust have been considered as indicators of a recent merger with other systems (e.g., Nieto & Bender 1989). These authors classify boxy ellipticals in three main types of galaxies which correlate with other physical properties: (i)

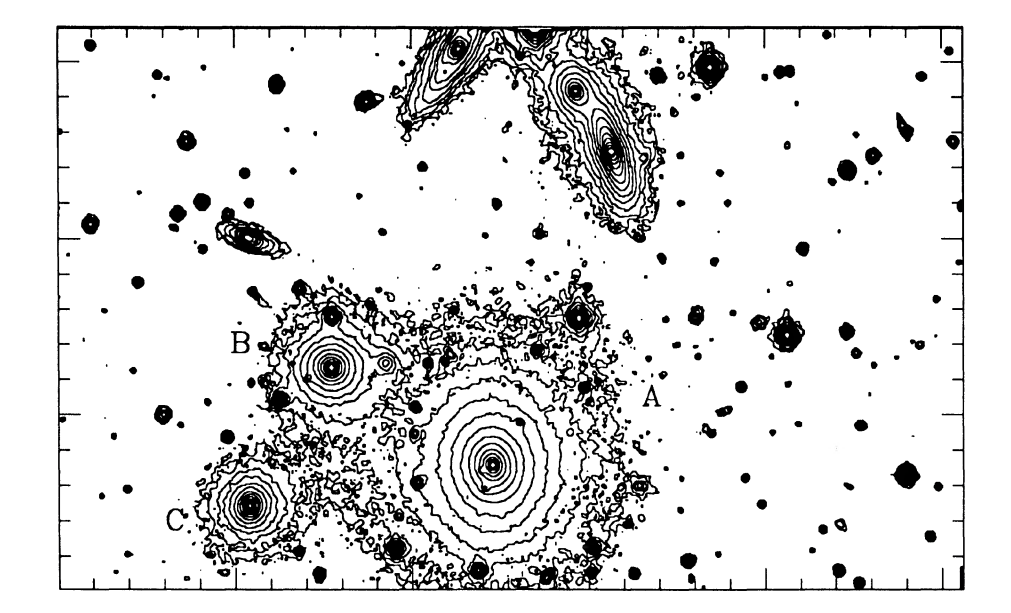


FIG. 7. Contour map of B2 2236+35 in the V filter. The lowest contour represents 25.0 mag arcsec⁻². The interval between contour is 0.5 mag. Orientation and scale are as in Fig. 1. Labels A, B, and C refer to the radio source and its companions, respectively.

pure boxy ellipticals, anisotropic and triaxial systems with signature of merging processes; (ii) low-mass, boxy galaxies, companions to massive galaxies, present indications of tidal truncation; (iii) boxy disk-ellipticals, with inner disk and outer boxiness, rotationally flattened and present no merging signatures. NGC 7052 belongs to the Bender's sample, from which this classification was constructed. However, this galaxy is not included in any of these groups. As the B₄ profile shows inner positive and outer negative values, we could classify it as boxy disk-E [class (iii)]. However, the properties of NGC 7052 are not in

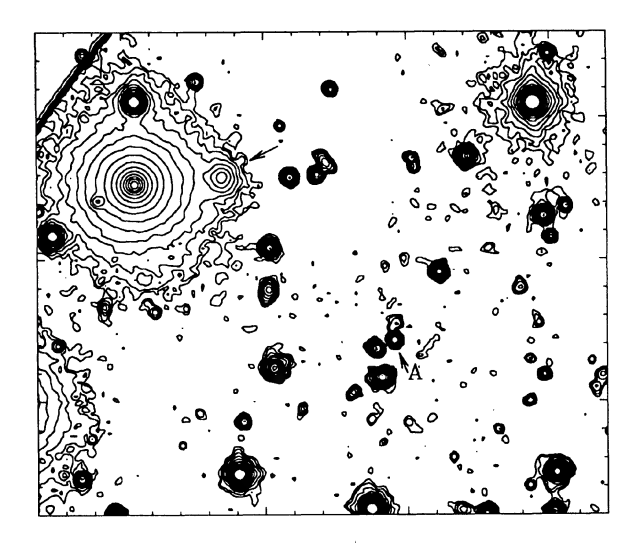


FIG. 8. Contour map of the residual image resulting after model subtraction in B2 2236+35. The interval between consecutive contours is 0.5 mag, and the lowest contour represents 25.6 mag arcsec². Letter A indicates the position of the nucleus and the arrow to the west of galaxy B indicates a faint extension detected. The separation between tick marks corresponds to 7".4.

agreement with the general properties of this class of boxy elliptical galaxies. On the other hand, the inner dust lane could contribute to the B₄ component and produce an irregular profile. In this case, NGC 7052 should be classified as a pure boxy elliptical with a central substructure. As suggested by Nieto *et al.* (1991) such separate structure may be formed in a merger event. A more detailed study of the inner part of NGC 7052 from high-resolution CCD imaging at the Nordic Optical Telescope will be given elsewhere (Pérez-Fournon & González-Serrano 1992).

The nature of the object detected near and parallel to the SW radio jet, at 9" from the nucleus, is difficult to clarify with the present data, but most probably it is not synchrotron emission from the jet because of the misalignment with the radio emission. A multicolor study or deep spectroscopy would be necessary to determine whether the emission represents strong star formation triggered by the jet, emission line regions associated with the radio emission or tidal debris resulting from a merging process.

4.1.3 B2 2236+25

The most interesting fact observed in B2 2236+35 is the presence of excesses over the de Vaucouleurs law that fitted the inner parts of the secondary galaxies. The excesses occur in the outer parts of these galaxies and start at levels of 22-23 mag arcsec⁻². This effect has been observed in pairs of elliptical galaxies (Paper I) and in other interacting systems (Lauer 1988), and is a strong indicator of tidal interaction (Aguilar & White 1986). The S-shaped morphology of the radio emission supports the interpretation of an ongoing gravitational encounter (Shaver et al. 1982). Aguilar & White (1986) made N-body simulations of galaxy encounters and conclude that galaxies having $r^{1/4}$ profiles maintain the profile after a close encounter with a

massive companion but with different slope. Furthermore, during the encounter, the brightness profile suffers variations. The core of strongly bound particles moves away from the center of mass of the outer particles. The result is that the inner parts follow the $r^{1/4}$ law but with decreasing effective radius during the encounter. Therefore, in the external parts, the profile presents an excess over the de Vaucouleurs law fitted to the central parts. The radius where the excess starts does not depend on encounter parameters but on the collision strength. The dynamical time at the distance where the boundary lies is equal to the time elapsed since the maximum approach. In the context of this model, it is possible to estimate this time, resulting in values of 1.2 and $2.4 \times 10^8 (M/L)^{-1/2}$ yr for galaxy B and C, respectively, where (M/L) is the mass-to-light ratio. These times must be taken as a simple approximation because this could be a three-galaxy encounter.

In summary, the five radio galaxies with radio jets studied here and in Paper I, show some kind of optical peculiarities that are currently taken as indicators of merging processes and interactions: presence of dust and underlying disks, boxy and/or disky isophotes, light excesses over the $r^{1/4}$ law, and isophote twisting, among others. In some cases, this interpretation is supported by the morphology of the radio source and by the location of the objects in high galaxy density regions. Colina & Pérez-Fournon (1990b) suggested that the differences in optical morphology, radio jet structure, infrared, and radio properties between multicomponent (i.e., one or more galaxies within a certain radius of the source) and isolated radio galaxies with jets are explained in terms of a different parent galaxy and interaction processes. In this context, gas-rich galaxies originate PRG and galaxies in interaction with a large elliptical originate a homogeneous class of LLRG. Isolate

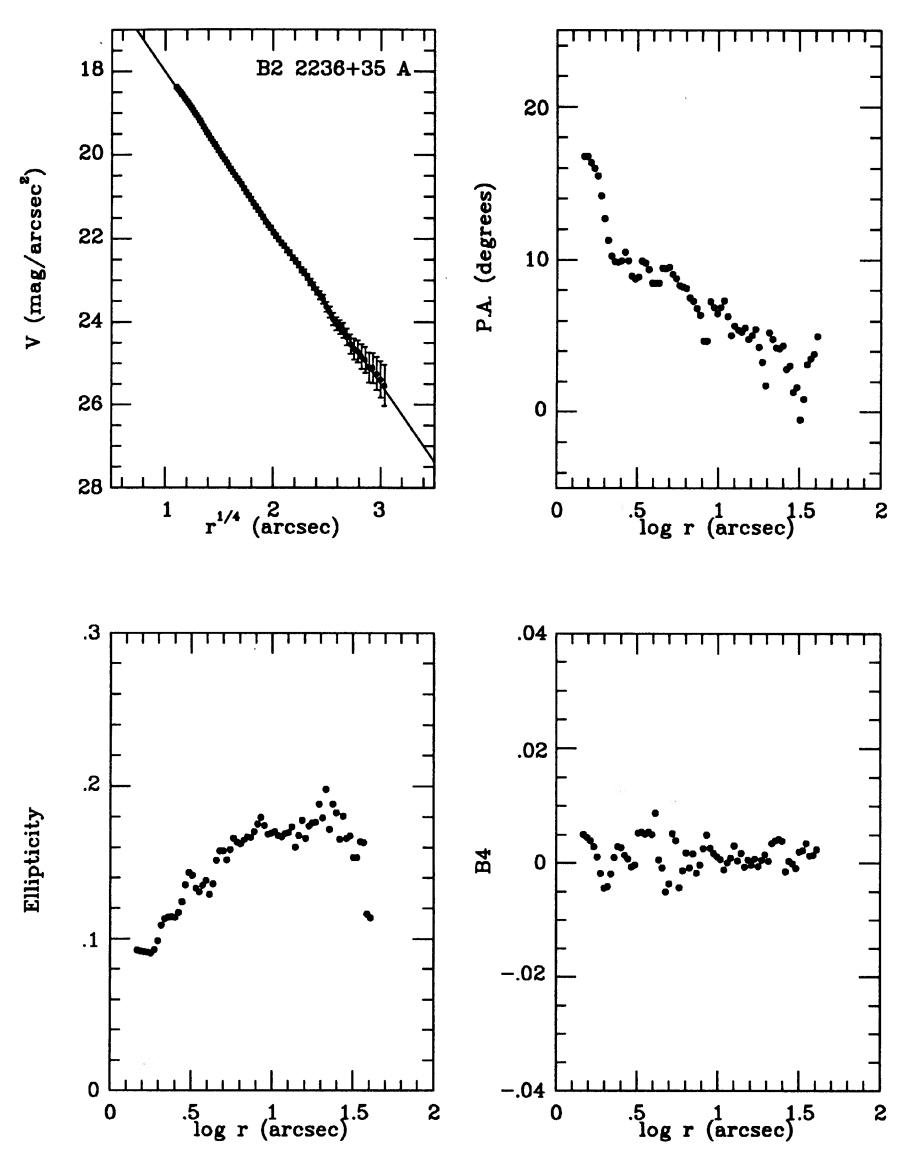


FIG. 9. Brightness profile and isophote parameters for the galaxies (a) B2 2236+35 A, (b) B, and (c) C. Solid lines are the fitted de Vaucouleurs law.

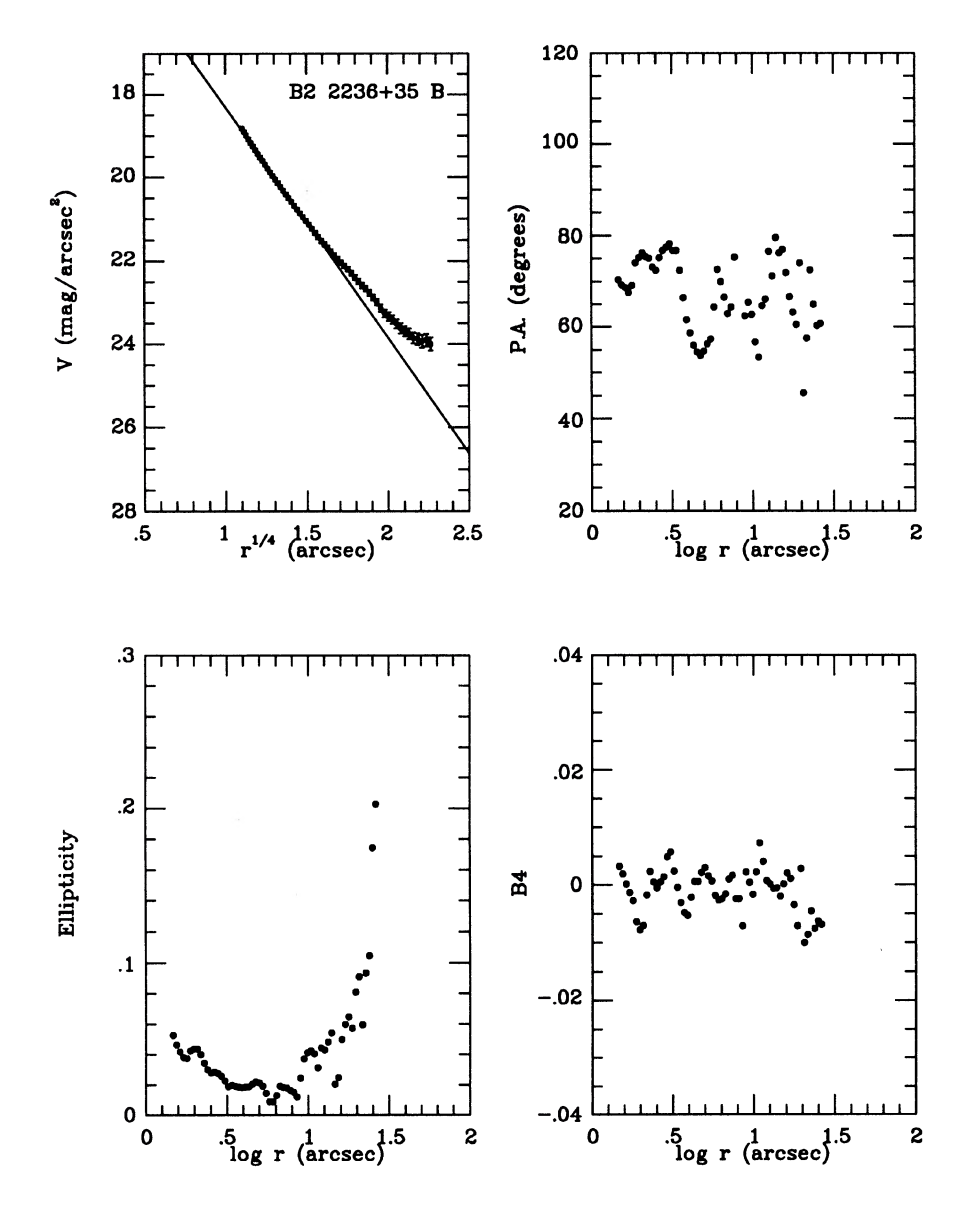


FIG. 9. (continued)

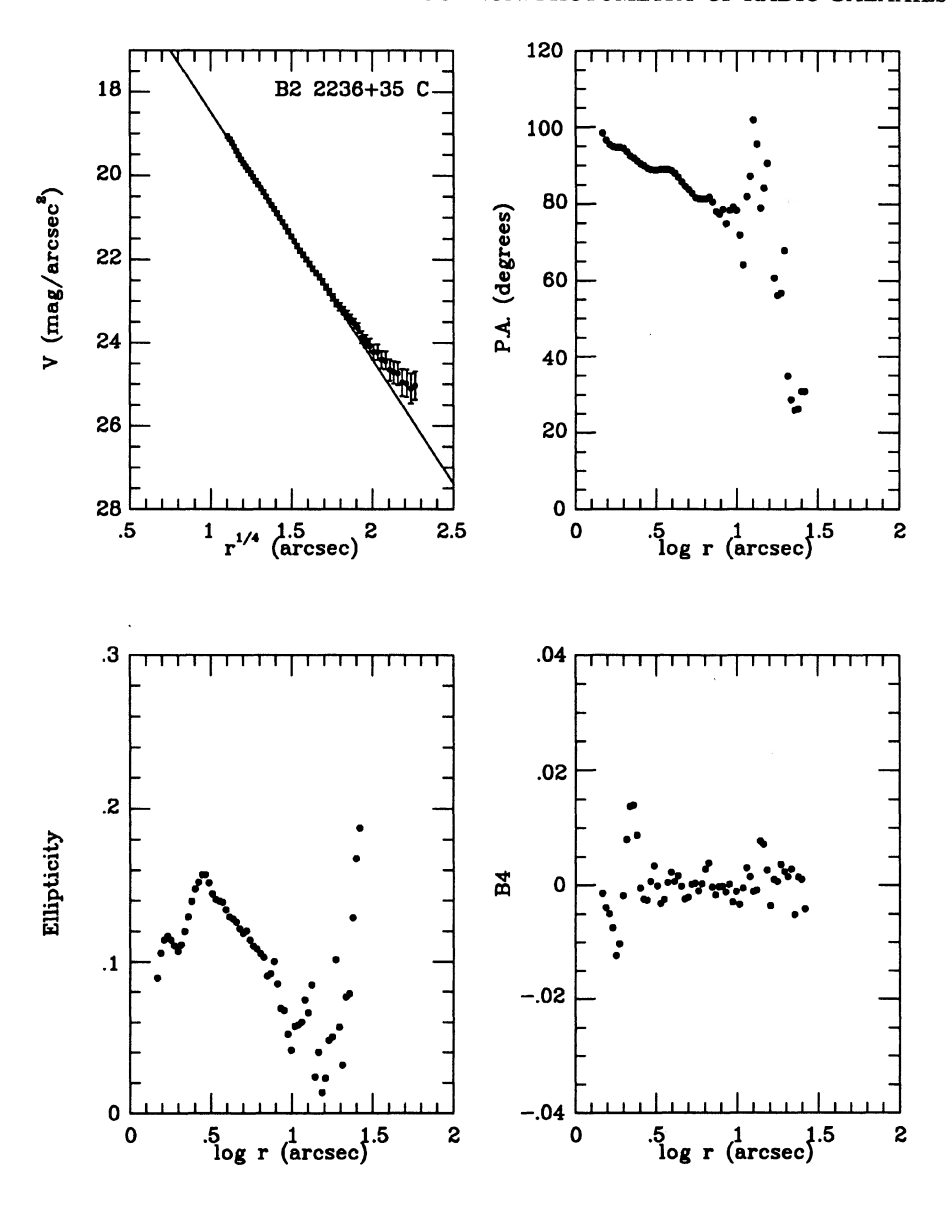


FIG. 9. (continued)

galaxies originate also LLRG but with heterogeneous properties. Three of the five galaxies discussed here belong to the sample studied by these authors. Our detailed analysis confirms the presence of interaction and merging events in these presumably gas-poor galaxies, and reinforces the idea of ongoing interaction processes between ellipticals as producing a well-defined class of radio jet sources.

4.2 Radio-to-Optical Spectral Index of the Jets

No optical counterpart of the radio jets has been detected. Our images, however, allow us to put strong limits to the radio-to-optical spectral indices of the jets. Bicknell et al. (1990) present surface-brightness profiles along the jet axis at a frequency of 1.4 GHz for a sample of B2 radio galaxies. B2 0836+29 and B2 2116+26 belong to this sample. For B2 2236+35 we will take the mean surface

brightness given by Parma et al. (1987). Radio spectral indices for the jets are listed in Table 2.

In regions free of galaxy emission, the limiting magnitude in the V band is ~ 26 mag arcsec⁻², while in the inner regions, where the galaxy brightness is high, this limit is about 1 mag lower due to the increase in Poisson noise.

For the inner jet in B2 0836+29, the surface brightness given by Bicknell et al. (1990) is 2 mJy arcsec⁻² at 3"-5" and 0.4 mJy arcsec⁻² at 20"-40". This implies lower limits for the radio-to-optical spectral index, $\alpha_{1.4}^V$ ($S_v \propto v^{-\alpha}$, where S_v is the flux density at frequency v), of 0.70-0.65 for the inner and outer parts, respectively. For the jets in B2 2116+26, well inside the optical emission of the galaxy, the estimated lower limit for $\alpha_{1.4}^V$ is 0.70. We obtain a value of 0.8 for the lower limit of the spectral index of the jets in B2 2236+35.

Taking into account the cases of B2 0034+25 and B2

0206+35, discussed in Paper I, we obtain lower limits to the spectral indices between radio and optical frequencies in the range 0.7-0.9, which are typical values in extragalactic jets with optical counterparts (Smith *et al.* 1983; González-Serrano *et al.* 1989; Keel 1986; Fraix-Burnet & Nieto 1988). Comparing the spectral indices at radio wavelengths, these lower limits are indicative of a steepening of the spectra of the jets in B2 2116+26 and B2 2236+35, much more evident in the first case, where the spectral index increases by, at least, 0.25.

It is possible to estimate upper limits to the cutoff frequencies of the spectra of the jets by assuming simple synchrotron models. We have calculated synchrotron spectra for power-law energy distributions, with index corresponding to the observed spectral index at radio frequencies, and cutoffs at high energies. These model spectra have been

compared with the observed radio and optical (lower limits) flux densities. Upper limits of cutoff frequencies for the jets considered here and in Paper I are in the range 2–5 $\times 10^{14}$ Hz. Therefore, it seems that all jets behave similarly at optical wavelengths, having cutoff frequencies below 5 $\times 10^{14}$ Hz. Similar values have been estimated for detected (Keel 1988; Pérez-Fournon *et al.* 1988) and for undetected jets (Fraix-Burnet *et al.* 1991). Clearly, longer exposure times in the optical and infrared imaging are needed to draw any conclusion on the distribution of cutoff frequencies.

J. I. G.-S. wishes to thank the Kapteyn Astronomical Institute, where part of this work was done, and also the Spanish Ministry of Education and Science and the Institute de Astrofísica de Canarias for financial support.

REFERENCES

Aguilar, L. A., & White, S. D. M. 1986, ApJ, 307, 97 Baum, S. A., & Heckman, T. M. 1989a, ApJ, 336, 681 Baum, S. A., & Heckman, T. M. 1989b, ApJ, 336, 702 Bender, R., Döbereiner, S., & Möllenhoff, C. 1988, A&AS, 74, 385 Bender, R., Surma, P., Döbereiner, S., Möllenhoff, C., & Medejsky, R. 1989, A&A, 217, 35 Bicknell, G. V., de Ruiter, H. R., Fanti, R., Morganti, R., & Parma, P. 1990, ApJ, 354, 98 Binggeli, B. 1982, A&A, 107, 338 Colina, L., & Pérez-Fournon, I. 1990a, ApJS, 72, 41 Colina, L., & Pérez-Fournon, I. 1990b, ApJ, 349, 45 Colla, G., et al. 1975, A&AS, 20, 1 Davoust, E., & Prugniel, P. 1988, A&A, 201, L30 Fabian, A. C., Nulsen, P. E. J., & Canizares, C. R. 1982, MNRAS, 201, Fraix-Burnet, D., Golombek, D., Macchetto, F., Nieto, J.-L., Lelievre, G., Perryman, M. A. C., & di Serego Alighieri, S. 1991, AJ, 101, 88 Fraix-Burnet, D., & Nieto, J.-L. 1988, A&A, 198, 87 Gallagher, J. S. 1986, PASP, 98, 81 González-Serrano, J. I. 1989, Ph.D. thesis, University of La Laguna González-Serrano, J. I., & Pérez-Fournon, I. 1989, ApJ, 338, L29 González-Serrano, J. I., Pérez-Fournon, I., Junor, W., & Spencer, R. 1989, Ap&SS 157, 183 González-Serrano, J. I., & Pérez-Fournon, I. 1991, A&A, 249, 75 (Paper Heckman, T. M., et al. 1986, ApJ, 311, 526 Jedrzejewski, R. I. 1987, MNRAS, 226, 747 Jura, M. 1986, ApJ, 306, 483 Keel, W. C. 1986, ApJ, 302, 296

Keel, W. C. 1988, ApJ, 329, 532 Lauer, T. R. 1988, ApJ, 325, 49 Morganti, R., Fanti, C., Fanti, R., Parma, P., & de Ruiter, H. R. 1987, A&A, 183, 203 Morganti, R., Fanti, R., Gioia, I. M., Harris, D. E., Parma, P., & de Ruiter, H. R. 1988, A&A, 189, 11 Nieto, J.-L., & Bender, R. 1989, A&A, 215, 266 Nieto, J.-L., Bender, R., & Surma, P. 1991, A&A, 244, L37 Ostriker, J. P., & Tremaine, S. D. 1975, ApJ, 202, L113 Owen, F. N., Rudwick, L., & Peterson, B. M. 1977, AJ, 82, 777 Parma, P., Fanti, C., Fanti, R., Morganti, R., & de Ruiter, H. R. 1987, A&A, 181, 244 Peletier, R. F. 1989, Ph.D. thesis, University of Groningen Pérez-Fournon, I., Colina, L., González-Serrano, J. I., & Biermann, P. L. 1988, ApJ, 329, L81 Pérez-Fournon, I., & González-Serrano, J. I. 1992, in preparation Schombert, J. M. 1987, ApJS, 64, 643 Schombert, J. M. 1988, ApJ, 328, 475 Shaver, P. A., et al. 1982, in Extragalactic Radio Sources, IAU Symposium No. 97, edited by D. J. Heeschen and C. M. Wade (Reidel, Dordrecht), p. 55 Smith, E. P., & Heckman, T. M. 1989a, ApJS, 69, 365 Smith, E. P., & Heckman, T. M. 1989b, ApJ, 341, 658 Smith, R. M., Bicknell, G. V., Hyland, A. R., & Jones, T. J. 1983, ApJ, Valentijn, E. A. 1979, A&AS, 38, 319 Wagner, S. J., Bender, R., & Möllenhoff, C. 1988, A&A, 195, L5 Zwicky, F., & Kowal, C. T. 1968, Catalogue of Galaxies of Clusters of

Galaxies (California Institute of Technology, Pasadena), Vol. 2